



An experimental study of the nanofluid pool boiling on the aluminium surface

Ahmad Nazari¹ · Seyfolah Saedodin²

Received: 7 February 2018 / Accepted: 29 July 2018 / Published online: 16 August 2018
© Akadémiai Kiadó, Budapest, Hungary 2018

Abstract

Nucleate boiling due to use latent heat instead of sensible heat has an extra potential for dissipating high heat flux, but it needs to control critical heat flux. On the other hand, it is well known that nucleate boiling is strongly under the influence characteristics of surface. One of the methods to control critical heat flux is to change surface characteristics by nanofluid pool boiling. In this study, nanofluids which contain aluminium oxide nanoparticles with four different levels of concentration including 0.002, 0.01, 0.05 and 0.1 vol% were used for pool boiling tests at the atmospheric pressure. Tests showed that generally to add nanoparticles will cause the critical heat flux increase and at the certain concentrations about 0.01 vol%, critical heat flux has maximum enhancement about 19%. In this research, additionally, the effects of surface parameters such as wettability, roughness and thickness of deposited nanoparticles on the critical heat flux have been analysed.

Keywords Critical heat flux · Pool boiling · Nanofluids · Wettability

List of symbols

g (m s^{-2})	Acceleration of gravity
ρ (kg m^{-3})	Density
ρ_l (kg m^{-3})	Liquid density
ρ_g (kg m^{-3})	Vapour density
σ (N m^{-1})	Surface tension
h_{fg} (J kg^{-1})	Latent heat of evaporation
K ($\text{W m}^{-1}\text{K}^{-1}$)	Thermal conductivity
q'' (W m^{-2})	Heat flux
vol%	Volume per cent
ΔT_{sat} (K)	Wall superheat temperature
θ (deg)	Contact angle
CHF (W m^{-2})	Critical heat flux
DW	Deionized water
T_w (K)	Surface temperature
γ_{sl} (N m^{-1})	Surface energy of solid–liquid
γ_{sv} (N m^{-1})	Surface energy of solid–liquid

T_1 (K)	Bulk temperature of liquid
T_2 (K)	Temperature of the first thermocouple in the conduction block
T_3 (K)	Temperature of the second thermocouple in the conduction block
T_4 (K)	Temperature of the third thermocouple in the conduction block

Introduction

The use of boiling phenomenon, which involves phase change of fluid and utilizes latent heat of vaporization for phase change and heat transfer, is an effective method for dissipating heat in devices with high thermal power. However, the boiling has inherent limitations, i.e. film boiling. The reason is the fact that when heat flux coming into the surface increases and the bubble generation rate on the surface is more than the bubble departure rate from the surface, a stable layer of bubbles is formed on the surface, that prevents heat transfer from the surface to the fluid; consequently, it excessively raises the surface temperature and damages the surface. Amount of heat flux at this moment is named critical heat flux (CHF). Thus, in the many types of equipment which the boiling is employed for cooling, heat flux is maintained in a range much lower than the CHF and

✉ Ahmad Nazari
anazari@shahroodut.ac.ir
Seyfolah Saedodin
s_sadodin@semnan.ac.ir

¹ Department of Mechanical and Mechatronics Engineering, Shahrood University of Technology, Shahrood, Iran

² Department of Mechanical Engineering, Semnan University, Semnan, Iran

this decreases efficiency of boiling heat transfer in such systems. Therefore, enhancement of the CHF can increase efficiency and safety in such equipment [1].

Investigations carried out on enhancement of CHF and improve boiling performance are include modifying surface characteristics and thermo-physical properties of working fluid. To change properties of surface by roughening and coating surface by means of micro- and nanostructure material has been extensively studied [2–8]. Another effective method for increasing CHF is to add nanoparticles to common fluids such as water, ethylene glycol and refrigerants. Materials used for nanoparticles can be chemically stable metals (e.g. gold, silver, copper), metal oxides (e.g. alumina, zirconia, silica, titania) and carbon in various forms (e.g. diamond, graphite, carbon nanotubes, fullerene). Contrary to the milli- and microsize particle slurries explored in the past, that quickly settle and often clog the flow channels, in the nanofluids, due to the fact that the size of nanoparticles is relatively close to size of base fluid molecules, if nanofluids properly dispersed, they can make very stable suspensions with little erosion and gravitational deposit over long periods of time [9–15]. Recent studies of nanofluids boiling are summarized in Table 1. Some of the major studies on this issue are briefly introduced in the followings.

You et al. [16] measured enhancement in CHF (up to 200%) for water-based 0.005 g L^{-1} alumina (Al_2O_3) nanofluid compared with pure water. They also reported that the CHF enhancement was achieved by increasing nanoparticle concentration only for relatively small concentrations up to 0.1 g L^{-1} . Kim et al. [17] studied the pool boiling characteristics of dispersions of alumina, zirconia and silica nanoparticles in water and reported that a remarkable enhancement in CHF can be achieved at relatively low nanoparticle concentrations (low than 0.1 vol%).

CHF enhancement was also reported by Vassallo et al. [18] who measured 60% increase in CHF using water-based SiO_2 nanofluid 0.5 vol%. They also reported that particles sediment on the heating surface. Kim et al. [19] conducted pool boiling experiments of nanofluids with different concentrations of Al_2O_3 or TiO_2 nanoparticles using a 0.2 mm diameter cylindrical Ni–Cr wire under atmospheric pressure. Vazquez et al. [20] reported 250–300% enhancement in CHF using water-based SiO_2 nanofluid (0.2–0.4 vol%). Sulaiman et al. [21] measured 150–200% enhancement in CHF with Al_2O_3 , TiO_2 and SiO_2 nanofluids ($0.04\text{--}1 \text{ g L}^{-1}$).

The results demonstrated that the critical heat fluxes of different nanofluids are remarkably over than pure water. Scanning electron microscopic observation showed that during the pool boiling of nanofluids, a nanoparticle coating is deposited on the wire surface. The CHF of deionized water was measured on a wire which was coated during the pool boiling experiments of nanofluids. The CHF of pure water on the nanoparticle-coated wire was close to that of nanofluids pool boiling test. These results showed that the modification of the boiling surface by deposited nanoparticles is the main reason for CHF enhancement of nanofluids.

In this study, nanofluids which contain aluminium oxide nanopowder with four different levels of concentration including very low, low, moderate and high concentration were used for pool boiling test and measuring CHF. Then by measuring of surface characteristics, the effect of each one of these characteristics on CHF will be analysed.

Table 1 Summary of reviews on nanofluid pool boiling

References	Nanofluids	CHF enhancement
You et al. [16]	Al_2O_3 ($0\text{--}0.05 \text{ g L}^{-1}$, Pressure: 2.89 psia) Substrate: $1 \times 1 \text{ cm}^2$ polished copper, and platinum wire	200% for copper, 160% for the platinum wire
Kim et al. [19]	Al_2O_3 , TiO_2 (0.00001–0.1 vol%)	100%
Vazquez et al. [20]	SiO_2 (0.2–0.4 vol%)	250–300%
Sulaiman et al. [21]	Al_2O_3 , TiO_2 and SiO_2 ($0.04\text{--}1 \text{ g L}^{-1}$)	150–200%
Vafaei et al. [22]	Al_2O_3 (0.001–0.1 vol%)	50%
Shahmoradi et al. [23]	Al_2O_3 (0.001–0.1 vol%)	47%
Ahn et al. [24]	Al_2O_3 (0.001 vol%)	136%
Lee et al. [25]	Al_2O_3 ($10^{-4}\text{--}0.01$ vol%)	160%
Park et al. [26]	Al_2O_3 (0.01 vol%)	120%
Umesh et al. [27]	TiO_2 /water (0.002 wt%)	200%
Kim et al. [28]	Al_2O_3 /water (0.0001–0.01 vol%)	54%

Material and method

Preparation of samples

Figure 1 shows a machined aluminium sample, which is used for the boiling test in this research. Aluminium has desirable properties such as high thermal conductivity, good corrosive resistance, low density; thus, it is commonly used as material for heat transfer in cooling, air conditioning and refrigeration systems. The material used is aluminium alloy 7075. This type of aluminium alloy has a melting point of 635 °C and a thermal conductivity coefficient of 130 W (m K)^{-1} .

After machining and dimensional control of all samples, in order to eliminate any grease and oil remained on the surface of samples during the machining operation, they are completely cleaned from oils using acetone and then washed with deionized water. In order to attain a uniform initial surface for all samples, the flat surface of all samples, which has 10 millimetres in diameter, is polished by using a polisher machine and sand paper 1500.

Preparation of nanofluids

Alumina nanofluid is widely used in heat transfer process because it is a stable and has uniform suspension, and also its thermo-physical properties have been well-documented [29–31].

The procedure used for the preparation of nanofluid in this research is two-step method. In this method, in order to prepare nanofluids with four different levels concentration include 0.002, 0.01, 0.05 and 0.1 vol%, firstly the selected nanoparticles, that is aluminium oxide nanopowder, type γ with purity of 99% and with the average diameter 47 nm given from the manufacturer (USNANO), are weighted by the accurate digital scale and then poured into a certain volume of deionized water without any additive. An ultrasonic vibrator, Sonicator™ Q700, was used to directly disperse the dry nanoparticles into deionized water for about 2 h. Amplitude is set 30. (Amplitude or intensity is controlled from 1 to 100%.)

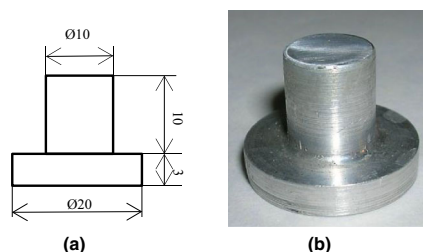


Fig. 1 **a** Dimensions of aluminium sample in millimetre, **b** picture of sample

The most common problem associated with utilizing nanofluids as the working fluid is sedimentation. In this research firstly, the used nanofluid has very low concentration. Secondly, for such dilute suspensions, the distance between particles is much larger than the particle size; thus, the forces and the interactions between particles at/near the liquid/gas interface have little impact on the surface energy. Thus, the van der Waals force between particles is weak. Additionally, it can be observed that turbulent during boiling due to formation, growth and collapse bubbles prevents the clustering and sedimentation of the nanoparticles [32–35].

Experimental set-up

Pool boiling experimental set-up has a cylindrical tank with a volume almost 700 cubic centimetres. As it is shown in Fig. 2, the wall of tank is made of Pyrex glass; thus, it is possible to observe the boiling phenomenon. The upper lid is made of aluminium and the lower lid from polytetrafluoroethylene (PTFE). The connection of upper and lower lids with the Pyrex tank is enabled by four long bolts and nuts.

In order to supply high heat flux, a copper heater is used and six cartridge heaters, each one with a diameter of 8 mm, a length of 4 cm, a power of 200 W, capable of generating a thermal power of 1200 W in total, are inserted into the holes made in the copper heater. In order to control heat flux, a power supply with voltage variation capability is used along with a multi-metre for measuring voltage or current.

As shown in Fig. 3, the aluminium sample is in contact with the copper heater from one end, which has a diameter of 20 mm, and is in contact with the fluid inside the tank from the other end, which has a diameter of 10 mm. At the contact location of the aluminium sample with the PTFE at the bottom of the tank, heat-resistance washers with commercial name of Green Great are used for sealing. Four type K thermocouples, namely T_1 , T_2 , T_3 and T_4 , are employed for temperature measurement in different points. T_1 is used for measuring the fluid temperature, T_2 for surface temperature, and T_3 and T_4 for heat flux. Each of these thermocouples has an exclusive sensor with 1 mm diameter. The wires of both ends of sensors are connected to a data logger device branded Lutron™, TM-947SD (Taiwan), which can display data on LCD and record data on a SD card.

Operating procedure and measurement

In the beginning of the experiment, almost 500 cubic centimetres of prepared nanofluids was poured into the Pyrex cylindrical tank. The auxiliary heater was then turned on in

Fig. 2 **a** A schematic diagram of experimental set-up for pool boiling test, **b** copper block and aluminium sample

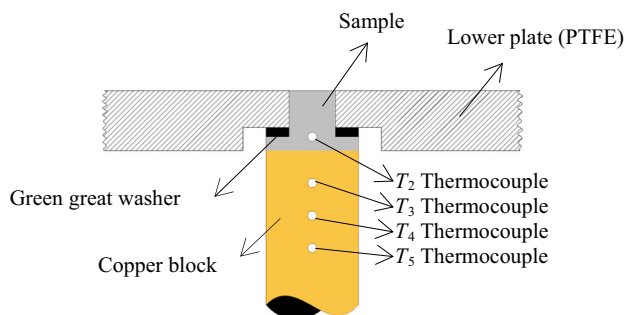
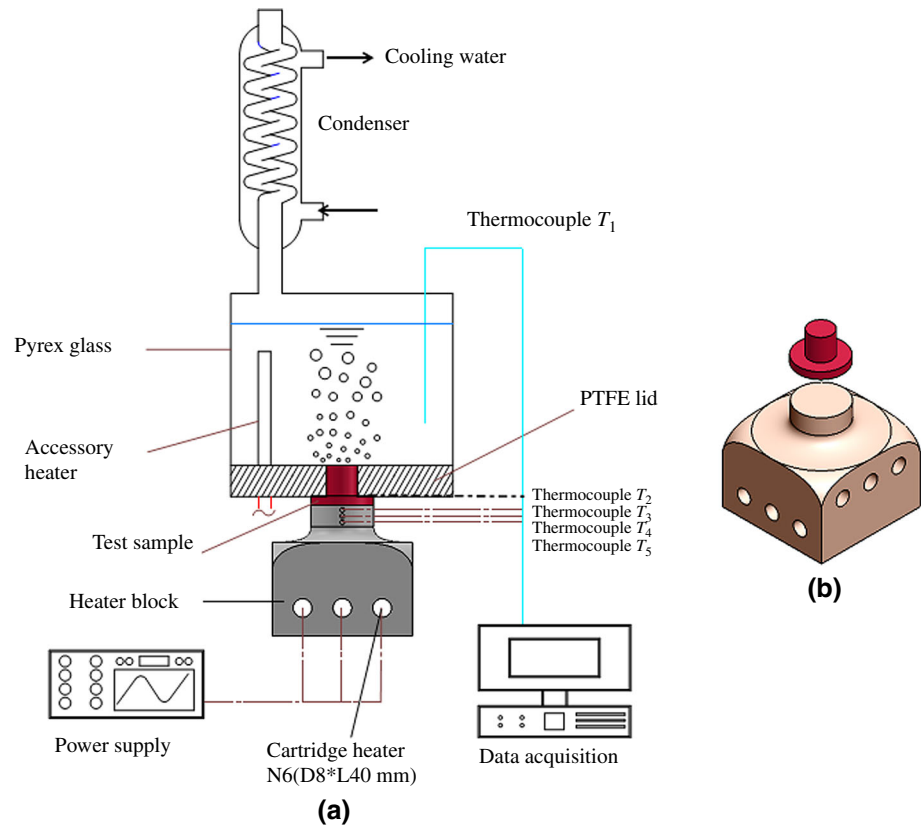


Fig. 3 Detail design of the test heater

order to increase the fluid temperature more quickly and to arrive at saturation temperature. Simultaneously, the main heater of the device was turned on and the voltage value was set on the minimum value possible for keeping the fluid at saturation temperature. After a while, the sample surface temperature increased and reached saturation temperature. As a result, vapour bubbles gradually started to appear on the surface of sample. When fluid temperature reached saturation temperature, auxiliary heater was turned off and in order to exit air bubbles from liquid, it was maintained at saturation temperature for 2 h. Then, the data logger system was switched on, so that the temperatures of T_1 , T_2 , T_3 and T_4 would be recorded in the memory. Data collection speed

could be set on the device. This value was equal to one data per second in this experiment.

Voltage was gradually increased at several stages. At each stage, once voltage had changed, 15 min was considered as the waiting period, so that steady-state conditions would be achieved. As voltage or heat flux was increased, the boiling regime gradually changed and a column of bubbles formed on the surface of sample. In the vicinity of the critical heat flux point, voltage variation had to be done very smoothly, otherwise excessive increase in the temperature of surface could damage to the sample. In the critical heat flux point, surface temperature abruptly increased over 100 degrees centigrade in less than three seconds, with a stable film of bubbles formed on the surface. Thus, as soon as the abrupt increase in temperature was observed, heat flux was stopped and the heater was turned off. The results of measured critical heat flux at various concentrations of nanofluids are shown in Table 1. These results are average three times run for boiling test in each concentration. In order to prevent heat losses and to measure the CHF more accurately, around the heater was covered by insulation and heat resistant material so that heat losses could be assumed negligible. All tests were carried out in atmospheric pressure and environment temperature (86 k Pa and 27 °C).

Assuming heat transfer in the top of the copper heater is one dimensional, and by measuring temperatures T_3 and T_4 ,

the heat flux can be calculated using Fourier’s law of heat conduction as follows:

$$q'' = K \frac{T_4 - T_3}{l} \tag{1}$$

Here, l is distance between thermocouples T_4 and T_3 and is equal with 7 mm.

The surface temperature T_w of aluminium sample can be extrapolated by measuring the temperature T_2 that is 10 mm lower than the surface of heater and using Fourier’s law of heat conduction.

$$T_w = T_2 - q'' \frac{\Delta}{k} \tag{2}$$

Here, Δ is 10 mm.

$$\Delta T_{\text{sat}} = T_w - T_{\text{sat}} \tag{3}$$

Uncertainties

The uncertainty of the measurement parameters is analysed by Kline and McClintock [36] method.

$$\frac{U_{q''}}{q''} = \sqrt{\left(\frac{U_k}{k}\right)^2 + \left(\frac{U_{\Delta T}}{T_4 - T_3}\right)^2 + \left(\frac{U_{\Delta x}}{\Delta x}\right)^2} \tag{4}$$

$$\frac{U_{T_w}}{T_w} = \sqrt{\left(\frac{U_{T_{\text{meas}}}}{T_w}\right)^2 + \left(\frac{1}{T_w} \cdot \frac{q''}{K} \cdot U_{\Delta x}\right)^2 + \left(\frac{1}{T_w} \cdot \frac{q'' \cdot \Delta x}{K^2} \cdot U_k\right)^2 + \left(\frac{\Delta U_{q''}}{T_w}\right)^2} \tag{5}$$

where the parameters $U_{q''}$, $U_{\Delta T}$, $U_{\Delta x}$ and U_k are the uncertainties of the heat flux, $T_4 - T_3$, Δx and thermal conductivity, respectively [37].

The error in the temperature and heat flux dissipated by the heater was estimated to be 0.5 °C and 4%, respectively. The error in the wall temperature and boiling heat flux with the copper block heater was estimated to be 0.5 °C and 5%, respectively. The maximum uncertainties in the wall temperature and heat flux measurements were within 4.7% and 6.8%, respectively.

Results and discussion

Calibration of set-up

In 1959, Zuber [4] developed a hydrodynamic model for prediction of the CHF on an infinite horizontal and smooth flat surface as follows:

$$q''_{\text{CHF}} = 0.131 h_{fg} \rho_g^{0.5} [\sigma g (\rho_l - \rho_g)]^{0.25} \tag{6}$$

where h_{fg} is latent heat of vaporization, σ is surface tension; ρ_l and ρ_g are liquid and vapour density, respectively.

Zuber’s model has good accuracy for DI water pool boiling test on the smooth flat surface. Therefore, this model is used for calibrating set-up by DI water. In order to calibrate pool boiling set-up, preliminary tests were performed using deionized water and a sample with smooth plate surface. Then, results were compared with Zuber’s well-known correlation at Eq. 6. Measured CHF from the test was 1034.2 kW m⁻², and the calculated amount using Zuber’s correlation was 1029.42 kW m⁻². This comparison showed that the amount of measured CHF was in a good agreement with Zuber’s correlation. Furthermore, this validation showed that experimental data obtained from pool boiling set-up could be reliable.

Boiling curves

One of the weaknesses of Zuber’s model was that, he did not consider the effect of surface properties. Following him, Kandlikar [38] proposed a model with considering the effect of surface wettability. It is for horizontal plate as follows:

$$q''_{\text{CHF}} = h_{fg} \rho_g^{0.5} \left(\frac{1 + \cos \theta}{16}\right) \left[\frac{2}{\pi} + \frac{\pi}{4} (1 + \cos \theta)\right]^{0.5} [\sigma g (\rho_l - \rho_g)]^{0.25} \tag{7}$$

Measured results of CHF and correlated by Kandlikar’s model are shown in Table 2. It is well known that wettability has significant effect on the CHF, but as will explained, in addition to wettability other parameters such as roughness, thickness and porosity of deposited layer are effective in the critical heat flux. Therefore, results obtained from Kandlikar’s model in Table 1, due to don’t consider effect each of these parameters, are different from measured results.

As shown in Fig. 4, at very low concentration, 0.002 vol%, due to very thin thickness of deposited nanoparticles, contact angle is almost same surface of initial sample, and therefore, CHF is almost same DW boiling test. At boiling test with the very low concentration of nanoparticles due to deposit very little nanoparticles and

Table 2 Measured critical heat flux at different concentrations of nanofluids

Concentration/vol%	CHF/W cm ⁻²	
	Measured	Kandlikar’s correlation
0 (DW)	103.42	78.82
0.002	107.1	88.56
0.01	121.18	138.4
0.05	114.6	145.74
0.1	115.8	152.78

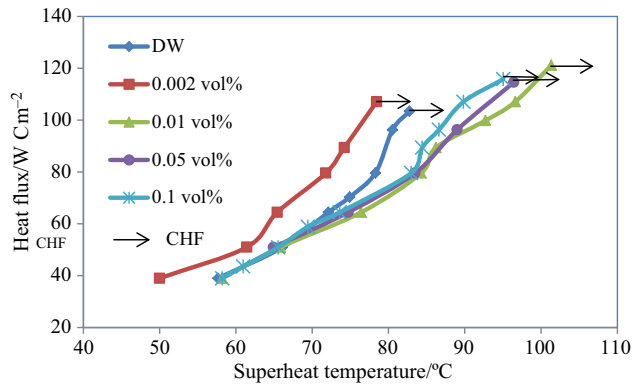


Fig. 4 Heat flux versus superheat temperature of surface for DW water and nanofluids

do not fill nucleation sites therefore, nucleation sites will activate earlier and superheat temperature of the surface is lower. But at higher concentrations due to fill nucleation sites and reduce number of them, superheat temperature of surface will be higher.

Relative variations of CHF of nanofluids to deionized water versus concentration are shown in Fig. 5. As shown in this figure, very low concentrations of nanoparticles have not effect on the CHF. On the other hand, the use of nanofluids with high concentrations reduces relative CHF. Only at certain concentrations, around of 0.01 vol%, enhancement of the CHF up to 19% can be seen. This trend of CHF variation was further confirmed by the experimental studies of Kim et al. [39], Golubovic et al. [40] and Liu et al. [41, 42] with fairly difference due to experimental parameters such as the nanoparticle materials and shape of heater.

As shown in Fig. 6, pool boiling heat transfer coefficient of nanofluids at all concentrations except very low concentration, 0.002 vol%, is less than deionized water. At high concentrations due to the significant effects of deposited nanoparticles on the surface characteristics, it causes the heat transfer coefficient decrease. A layer of

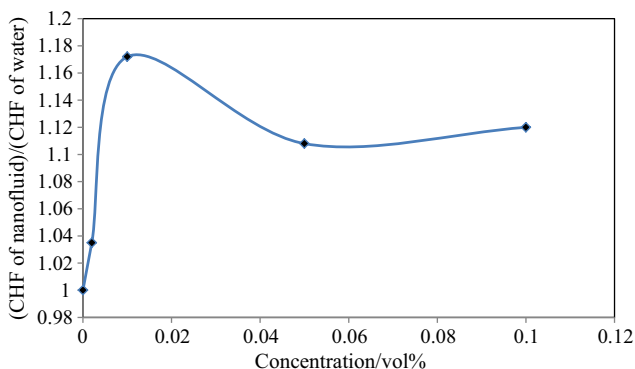


Fig. 5 Curve of relative variations of CHF of nanofluid to water versus concentration

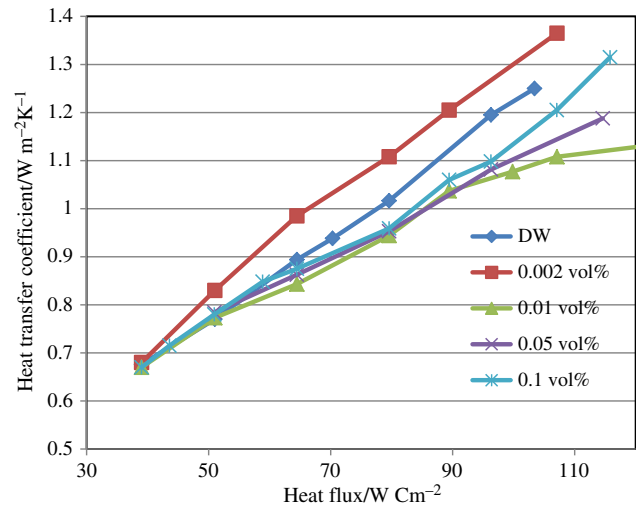


Fig. 6 Variations of pool boiling heat transfer coefficient with heat flux at different concentrations

nanoparticles deposited on the surface can decrease heat transfer coefficient. Because, firstly when nanoparticles deposit, they fill cavities on the surface and reduce nucleation site density. Secondly, thermal conductivity of deposited layer is very lower than aluminium sub-layer. Thickness of deposited layer is depended on concentration of nanofluid. Therefore, as shown in the Fig. 6 with increasing concentration, the heat transfer coefficient decreases. At very low concentration (0.002 vol%), because deposited nanoparticles are negligible and the effect of nanoparticles in the fluid is more dominant than deposited nanoparticles in the heat transfer, it has heat transfer coefficient higher than deionized water.

As shown in Fig. 5, extent of the variations in concentrations of less than 0.01 vol% is remarkable. Therefore, boiling phenomenon is more influenced by low concentrations of nanoparticles. In order to analyse these changes in boiling parameters, two factors can be considered: first, the change in chemical and thermo-physical properties of fluid due to adding nanoparticles and second, the change in geometrical properties of the surface due to deposit of nanoparticles on the boiling surface.

Dispersed nanoparticles in the deionized water are in the form of a suspension solution, and no reaction occurs between the nanoparticles and the base fluid. In addition, due to not using surfactants as well as the low volume fraction of nanoparticles, it can be concluded that the chemical composition and thermo-physical properties of nanofluids are approximately equal to the base fluid and will not change. This is confirmed in many tables and researches on properties of alumina nanofluid at low concentrations [34]. As shown in Fig. 7, Kwark et al. [43] measured thermo-physical properties of Al₂O₃ nanofluid as thermal conductivity, surface tension and viscosity at

low concentrations. Figure 7 summarizes these experimental results, and it can be concluded that nanofluids do not affect the thermal properties of base fluid (water) at the low concentrations ($\leq 1 \text{ g L}^{-1}$) tested.

Two factors have effect on the surface tension of nanofluid, surfactant and change in concentration due to evaporation of nanofluid. In this research because of, firstly don't use of surfactant and secondly use of condenser in order to the prevention of nanofluid vaporization and keep constant of concentration, surface tension will be constant [35]. Furthermore, at low particle concentrations, because for dilute nanofluids, the distance between particles is much larger than the particle size; thus, the forces and the interactions between particles at the liquid interface have little impact on the surface energy [34].

Therefore, first factor cannot be the reason for changing specifications of boiling and the main reason for changing is deposition of the nanoparticles on the surface. The effect of deposited nanoparticles on the surface can be determined by measuring the parameters of boiling surface such as roughness, wettability and coating thickness. The results obtained from the measurement of the surface parameters and their effects on the critical heat flux will be explained in the following.

Parameters of surface

After the boiling tests, all samples were analysed accurately. At the first glance, it was observed that a thin layer of aluminium oxide nanoparticles was deposited on the

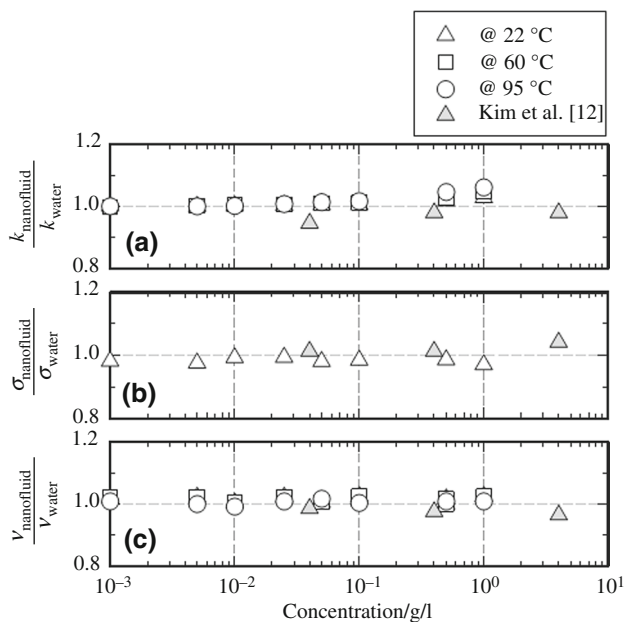


Fig. 7 Thermo-physical properties of Al_2O_3 nanofluids at various concentrations and temperatures. **a** Thermal conductivity, **b** surface tension and **c** kinematic viscosity [43]

surface uniformly. It must be noted that deposition of nanoparticles at this state is not gravitational deposition or sedimentation because if tank has been upside-down, nanoparticles could not be separated from surface and back to fluid, because they are bonded to surface. Deposition of nanoparticles is due to vaporize liquid in the microlayer region beneath the bubble. As liquid in the microlayer vaporize, bubble grows and concentration of nanoparticles in this region increases. Nanoparticles come closer, and regard to high temperature of the surface, they bond to the hot heater surface [43]. In this layer of deposited nanoparticles on the boiling surface, due to porosity and high absorbency of alumina nanoparticles, wettability increases and also owing to porosity of this layer, capillary wicking flow within this layer increases too. Both of these factors will prevent to dry out surface and will delay CHF [44, 45].

The effect of contact angle

As shown in Fig. 8, static contact angle of samples was measured by drop shape analysis (DSA) method. The video-based optical contact angle measuring system, DataphysicsTM, OCA 15 EC (England) was used for measuring contact angle. The contact angle was measured five times for each sample. Tests were carried out at an ambient laboratory temperature $27 \text{ }^\circ\text{C}$ and at relative humidity 55%. Angle between the baseline of the drop and the tangent at the drop boundary is measured.

At the nucleate boiling, maximum heat flux is limited to CHF by the mechanisms of liquid supply to and vapour escape from the phase-change interface [46]. Many nanofluid boiling studies have shown that the improvement of surface wettability by depositing nanoparticle can increase the CHF [47].

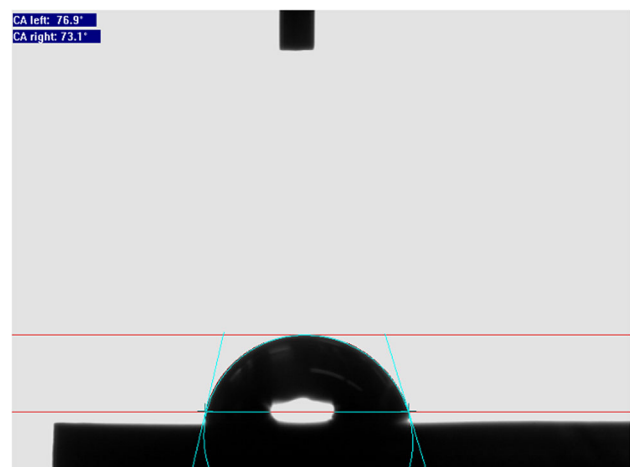


Fig. 8 Measurement of contact angle by drop shape analysis method. Uncertainty is about $\pm 0.1^\circ$

Deposition of nanoparticles is due to vaporize liquid in the microlayer area under the bubble. As liquid in the microlayer vaporize, bubble grows and concentration of nanoparticles in this area increases. Nanoparticles come closer, and regard to high temperature of the surface, nanoparticles bond to the hot heater surface [43]. In this layer of deposited nanoparticles on the boiling surface, due to high absorbency of alumina nanoparticles, wettability increases and also owing to porosity of this layer, capillary wicking flow within this layer increases too. Both of these factors will cause surface immediately rewets, and thus, it will prevent to dry out surface and will delay CHF.

As shown in Figs. 9 and 10, in very low concentration of nanoparticles, 0.002 vol%, due to deposit a very thin layer of nanoparticles, contact angle changes a little. But with increasing concentration to low concentration, 0.01 vol%, the thickness of deposited layer increases remarkably and this will cause contact angle to decrease significantly. Therefore, in this condition CHF will increase remarkably. Furthermore, it is noticeable that in this situation, roughness increases too and this can be effective in more enhancement of the critical heat flux. At concentrations more than 0.01 vol%, although thickness has increased, roughness and CHF have decreased unexpectedly and this needs more investigations.

The effect of coating thickness

Thickness of deposited nanoparticles layer on the surface of sample was measured by a Thickness-metre device ElcometerTM, 456. Thickness of deposited layer is depended on concentration and boiling duration. As regards, boiling duration for all samples has been same; therefore, it can be concluded that thickness is depended on concentration of nanoparticles. Results in Table 2 confirm this subject. On the other hand, with increasing thickness, wettability of surface will increase, and at high thickness, variation in the wettability will be less. Based on experiments done by Kwark et al. [43] at the certain thickness,

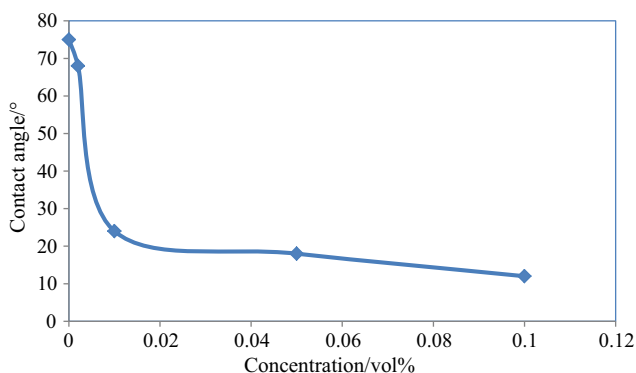


Fig. 9 Curve of contact angle versus concentration

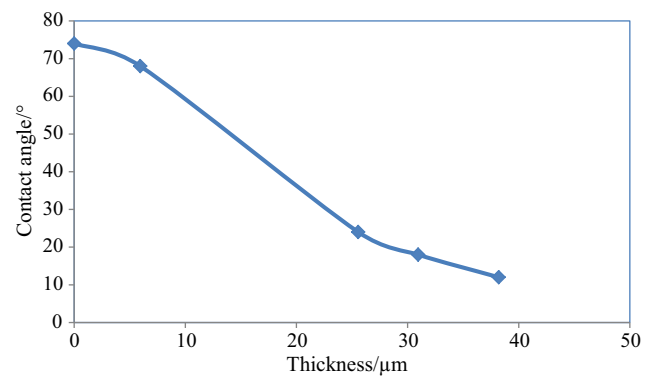


Fig. 10 Curve of thickness versus contact angle

wettability will be the maximum value and after that with increasing thickness, wettability will remain constant. In order to determine the optimum thickness, more experiments must be done.

The effect of roughness

After boiling test, roughness of all samples was measured. Results obtained from the measurement of surface roughness using atomic force microscopic device NT-MDTTM, NTEGRA (Russia) are shown in Fig. 11. As shown in this figure, the highest roughness of the surface is related to the sample tested by nanofluids with a concentration of 0.01 vol%. This sample has highest critical heat flux. Therefore, it can be concluded that surface roughness has a direct effect on the critical heat flux. Because regard to Young's equation that was modified by Wenzel [48] as follows:

$$\cos\theta = \frac{\gamma_{sv} - \gamma_{sl}}{\sigma} r \quad (8)$$

This equation shows relation contact angle, θ to surface tension, σ , adhesion tension, $\gamma_{sv} - \gamma_{sl}$ and roughness. Wenzel defined a roughness factor, r , as the ratio of the effective contact area to the smooth contact area. According to the above equation with increasing surface roughness, contact angle decreases. It is well known that decrease in contact angle will increase critical heat flux [49].

According to the results obtained in Figs. 5 and 9, in the concentrations of average and above, although wettability increases, critical heat flux reduces; therefore, it can be concluded that in addition to wettability, another parameter is effective on the critical heat flux. As shown in Figs. 4 and 12 with the exception of very small concentration, 0.002 vol%, the trend of changing of roughness is similar to the trend of changing of critical heat flux at different concentrations. In other words, by increasing or decreasing the concentration, the critical heat flux and roughness

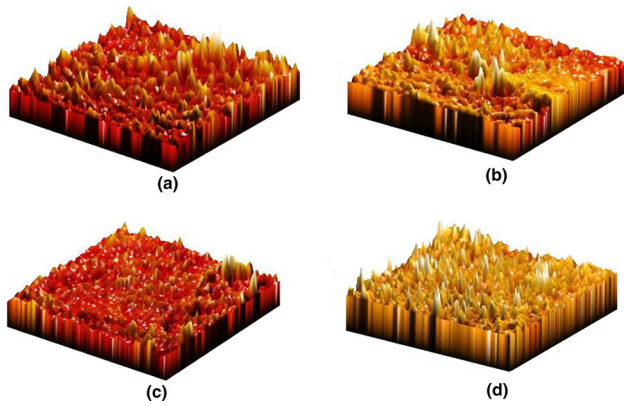


Fig. 11 Three-dimensional pictures and amounts of roughness of surface. **a** Boiling by nanofluid 0.002 vol%. $R_a = 0.147 \mu\text{m}$, $R_{\text{rms}} = 0.2 \mu\text{m}$, **b** boiling by nanofluid 0.01 vol%. $R_a = 0.326 \mu\text{m}$, $R_{\text{rms}} = 0.433 \mu\text{m}$, **c** boiling by nanofluid 0.05 vol%. $R_a = 0.228 \mu\text{m}$, $R_{\text{rms}} = 0.335 \mu\text{m}$, **d** boiling by nanofluid 0.1 vol%. $R_a = 0.221 \mu\text{m}$, $R_{\text{rms}} = 0.313 \mu\text{m}$

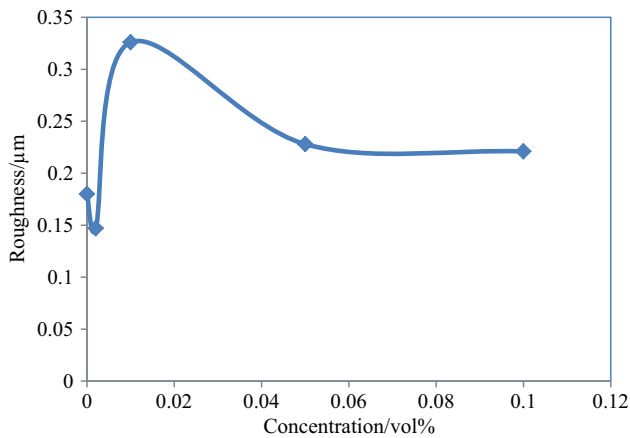


Fig. 12 Curve of roughness versus concentration

changes similarly. Therefore, it can be concluded that the critical heat flux in addition to being directly influenced by wettability it is affected by roughness.

Conclusions

In this paper, it was shown that during nanofluid pool boiling process, a layer of nanoparticles is deposited on the boiling surface. The effect of deposited nanoparticles on the surface was determined by measuring the parameters of boiling surface such as roughness, wettability and coating thickness. It was founded that deposited nanoparticles can change morphological and chemistry characteristics of surface such as roughness and wettability. This will cause main parameters of boiling change significantly. It was concluded that deposition of nanoparticles increases

wettability and this is main reason enhancement of CHF. Furthermore, very low concentrations of nanoparticles have no effect on the CHF and at certain concentrations; around 0.01 vol%, maximum enhancement of the CHF up to 19% was seen.

References

- Kandlikar SG. Handbook of phase change: boiling and condensation. Abingdon: Taylor & Francis; 1999.
- Kim DE, et al. Review of boiling heat transfer enhancement on micro/nanostructured surfaces. *Exp Thermal Fluid Sci.* 2015;66:173–96.
- Nazari A, Saedodin S. Porous anodic alumina coating for optimisation of pool-boiling performance. *Surf Eng.* 2017;33(10):753–9. <https://doi.org/10.1080/02670844.2016.1199187>.
- Kim JS, et al. Effect of surface roughness on pool boiling heat transfer of water on hydrophobic surfaces. *Int J Heat Mass Transf.* 2018;118:802–11.
- Kim J, et al. Effect of surface roughness on pool boiling heat transfer of water on a superhydrophilic aluminum surface. *J Heat Transf.* 2017;139(10):101501.
- Kim J, et al. Effect of surface roughness on pool boiling heat transfer at a heated surface having moderate wettability. *Int J Heat Mass Transf.* 2016;101:992–1002.
- Shojaeian M, et al. Investigation of change in surface morphology of heated surfaces upon pool boiling of magnetic fluids under magnetic actuation. *Mater Res Exp.* 2016;3(9):096102.
- Karimzadehkhoei M, et al. Stick and oscillatory behavior of bubbles due to TiO_2 nanoparticle coating in subcooled pool boiling on a wire. *Appl Phys Lett.* 2017;111(6):061601.
- Barber J, Brutin D, Tadrist L. A review on boiling heat transfer enhancement with nanofluids. *Nanoscale Res Lett.* 2011;6(1):1–16.
- Ahn HS, Kim MH. A review on critical heat flux enhancement with nanofluids and surface modification. *J Heat Transf.* 2012;134(2):024001.
- Dikici B, Eno E, Compere M. Pool boiling enhancement with environmentally friendly surfactant additives. *J Therm Anal Calorim.* 2014;116(3):1387–94.
- Vafaei S, Borca-Tasciuc T. Role of nanoparticles on nanofluid boiling phenomenon: nanoparticle deposition. *Chem Eng Res Des.* 2014;92(5):842–56.
- Phan HT, et al. Surface coating with nanofluids: the effects on pool boiling heat transfer. *Nanoscale Microscale Thermophys Eng.* 2010;14(4):229–44.
- Ciloglu D, Bolukbasi A. A comprehensive review on pool boiling of nanofluids. *Appl Therm Eng.* 2015;84:45–63.
- Hashemi M, Noie SH. Study of flow boiling heat transfer characteristics of critical heat flux using carbon nanotubes and water nanofluid. *J Therm Anal Calorim.* 2017;130(3):2199–209.
- You S, Kim J, Kim K. Effect of nanoparticles on critical heat flux of water in pool boiling heat transfer. *Appl Phys Lett.* 2003;83(16):3374–6.
- Kim S, et al. Surface wettability change during pool boiling of nanofluids and its effect on critical heat flux. *Int J Heat Mass Transf.* 2007;50(19):4105–16.
- Vassallo P, Kumar R, D'Amico S. Pool boiling heat transfer experiments in silica–water nano-fluids. *Int J Heat Mass Transf.* 2004;47(2):407–11.

19. Kim HD, Kim J, Kim MH. Experimental studies on CHF characteristics of nano-fluids at pool boiling. *Int J Multiph Flow*. 2007;33(7):691–706.
20. Vazquez DM, Kumar R. Surface effects of ribbon heaters on critical heat flux in nanofluid pool boiling. *Int Commun Heat Mass Transf*. 2013;41:1–9.
21. Sulaiman MZ, et al. Systematic measurements of heat transfer characteristics in saturated pool boiling of water-based nanofluids. *Int J Heat Mass Transf*. 2016;102:264–76.
22. Vafaei S, Wen D. Critical heat flux (CHF) of subcooled flow boiling of alumina nanofluids in a horizontal microchannel. *J Heat Transf*. 2010;132(10):102404.
23. Shahmoradi Z, Etesami N, Nasr M, Esfahany, Pool boiling characteristics of nanofluid on flat plate based on heater surface analysis. *Int Commun Heat Mass Transf*. 2013;47:113–20.
24. Ahn HS, Kim MH. The boiling phenomenon of alumina nanofluid near critical heat flux. *Int J Heat Mass Transf*. 2013;62:718–28.
25. Lee JH, Lee T, Jeong YH. The effect of pressure on the critical heat flux in water-based nanofluids containing Al_2O_3 and Fe_3O_4 nanoparticles. *Int J Heat Mass Transf*. 2013;61:432–8.
26. Park SD, Moon SB, Bang IC. Effects of thickness of boiling-induced nanoparticle deposition on the saturation of critical heat flux enhancement. *Int J Heat Mass Transf*. 2014;78:506–14.
27. Umesh V, Raja B. A study on nucleate boiling heat transfer characteristics of pentane and CuO-pentane nanofluid on smooth and milled surfaces. *Exp Therm Fluid Sci*. 2015;64:23–9.
28. Kim JH, et al. Effect of aluminum oxide and reduced graphene oxide mixtures on critical heat flux enhancement. *Int J Heat Mass Transf*. 2018;116:858–70.
29. Zhu D, Wu S, Wang N. Thermal physics and critical heat flux characteristics of Al_2O_3 - H_2O nanofluids. *Heat Transf Eng*. 2010;31(14):1213–9.
30. Teng T-P, Hung Y-H. Estimation and experimental study of the density and specific heat for alumina nanofluid. *J Exp Nanosci*. 2014;9(7):707–18.
31. Lee J-H, et al. Effective viscosities and thermal conductivities of aqueous nanofluids containing low volume concentrations of Al_2O_3 nanoparticles. *Int J Heat Mass Transf*. 2008;51(11–12):2651–6.
32. Karimzadehkhoei M, et al. The effect of nanoparticle type and nanoparticle mass fraction on heat transfer enhancement in pool boiling. *Int J Heat Mass Transf*. 2017;109:157–66.
33. Şeşen M, et al. Boiling heat transfer enhancement of magnetically actuated nanofluids. *Appl Phys Lett*. 2013;102(16):163107.
34. Tanvir S, Qiao L. Surface tension of nanofluid-type fuels containing suspended nanomaterials. *Nanoscale Res Lett*. 2012;7(1):226.
35. Chen R-H, Phuoc TX, Martello D. Surface tension of evaporating nanofluid droplets. *Int J Heat Mass Transf*. 2011;54(11–12):2459–66.
36. Kline SJ, McClintock F. Describing uncertainties in single-sample experiments. *Mech Eng*. 1953;75(1):3–8.
37. Holman JP. *Experimental methods for engineers*. New York: McGraw-Hill; 1966.
38. Kandlikar SG. A theoretical model to predict pool boiling CHF incorporating effects of contact angle and orientation. *J Heat Transf*. 2001;123(6):1071–9.
39. Kim H, Kim M. Experimental study of the characteristics and mechanism of pool boiling CHF enhancement using nanofluids. *Heat Mass Transf*. 2009;45(7):991–8.
40. Golubovic MN, et al. Nanofluids and critical heat flux, experimental and analytical study. *Appl Therm Eng*. 2009;29(7):1281–8.
41. Liu Z-H, Xiong J-G, Bao R. Boiling heat transfer characteristics of nanofluids in a flat heat pipe evaporator with micro-grooved heating surface. *Int J Multiph Flow*. 2007;33(12):1284–95.
42. Liu Z-H, Liao L. Sorption and agglutination phenomenon of nanofluids on a plain heating surface during pool boiling. *Int J Heat Mass Transf*. 2008;51(9):2593–602.
43. Kwark SM, et al. Pool boiling characteristics of low concentration nanofluids. *Int J Heat Mass Transf*. 2010;53(5):972–81.
44. Kiyomura I, et al. An analysis of the effects of nanoparticles deposition on characteristics of the heating surface and ON pool boiling of water. *Int J Heat Mass Transf*. 2017;106:666–74.
45. Salimpour MR, Abdollahi A, Afrand M. An experimental study on deposited surfaces due to nanofluid pool boiling: comparison between rough and smooth surfaces. *Exp Therm Fluid Sci*. 2017;88:288–300.
46. Liter SG, Kaviany M. Pool-boiling CHF enhancement by modulated porous-layer coating: theory and experiment. *Int J Heat Mass Transf*. 2001;44(22):4287–311.
47. Zhang F, Jacobi AM. Nanoparticle deposition by boiling on aluminum surfaces to enhance wettability. In: *International Refrigeration and Air Conditioning Conference*. Paper 1468. 2014. <http://docs.lib.purdue.edu/iracc/1468>.
48. Wenzel RN. Surface roughness and contact angle. *J Phys Chem*. 1949;53(9):1466–7.
49. O'Hanley H, et al. Separate effects of surface roughness, wettability, and porosity on the boiling critical heat flux. *Appl Phys Lett*. 2013;103(2):024102.